Available online at www.CivileJournal.org

Civil Engineering Journal

(E-ISSN: 2476-3055; ISSN: 2676-6957)

Vol. 9, No. 12, December, 2023

Modeling Finned Thermal Collector Construction Nanofluid-based Al_2O_3 to Enhance Photovoltaic Performance

Singgih D. Prasetyo [1], Eko P. Budiana [1], Aditya R. Prabowo [1], Zainal Arifin [1*]

[1] *Department of Mechanical Engineering, Faculty of Engineering, Universitas Sebelas Maret, Surakarta,57126 Indonesia.*

Received 30 July 2023; Revised 09 November 2023; Accepted 14 November 2023; Published 01 December 2023

Abstract

Extensive research has been conducted to address the issue of the reduced efficiency of solar photovoltaic (PV) cells at high temperatures. To address this problem, a hybrid cooling system has been developed. This system uses a thermal collector to convert waste heat into reusable heat. Selecting the best configuration and operational parameters for the collector is crucial for maximizing system performance. To achieve this, we conducted computational fluid dynamics (CFD) modeling using ANSYS. Various factors affecting the cooling of PV solar cells were analyzed, including the collector design, mass flow rate, and concentration of the Al_2O_3 nanofluids. Results showed that the 12S finned thermal collector system exhibits the lowest temperature for PV solar cells, at approximately 29.654 °C. The electrical efficiency of PV solar cells is influenced by the concentration of Al_2O_3 nanofluids. We found that the 12S finned collector system with 1% water/Al_2O_3 nanofluid achieved the highest efficiency (approximately 11.749%) at a flow rate of 0.09 kg/s. The addition of finned collectors affects efficiency and variations in fluid mass flow rates, and there is no relation between the connector type and different Al_2O_3 nanofluid concentrations. In other words, the cooling system can be optimized to enhance the efficiency of the PV solar cells under high-temperature conditions.

Keywords: PV; CFD; ANSYS; Finned Thermal Collector; Efficiency.

1. Introduction

Photovoltaic (PV) solar cells have gained widespread popularity as viable alternatives for electricity generation. They harness abundant renewable energy resources provided by solar radiation. These cells function by converting incoming sunlight into electrical energy by utilizing the PV effect. The efficiency of PV cells typically falls within 10%–16%. This efficiency range is influenced by various factors, including the specific wavelengths of light absorbed and converted into electricity [1, 2]. However, a portion of solar energy remains unused, reducing the efficiency of the PV solar cell. As the temperature increases, the electrical output of the cell decreases, leading to a decrease in cell efficiency. When crystalline silicon PV solar cells operate at temperatures above 25°C, they experience a temperature-related power loss with coefficients ranging from 0.4 to 0.65%/K [3, 4].

Over the last decade, extensive research has been conducted to address the negative effects of elevated temperatures on PV cells. The increase in the solar cell temperature can be categorized in several ways, including radiant [5], convection [6], and conductive heat extraction techniques [7]. To solve this problem, hybrid systems have been developed by converting waste heat into productive heat using solar collectors [8]. These studies employed mechanical and electrical mechanisms, with the mechanical solutions relying primarily on fluid circulation [9]. Fluid circulation techniques include air [10], water [11], nanofluids [12], and phase-change materials (PCM) within the collectors of PV

* Corresponding author: zainal_arifin@staff.uns.ac.id

http://dx.doi.org/10.28991/CEJ-2023-09-12-03

solar cell cooling systems [13]. Investigations were conducted under unconcentrated or concentrated solar radiation using technical features such as the glass effect and finned channels [14, 15].

Similar to flat plate collectors, solar collectors can heat fluids to temperatures up to 100 °C higher than the surrounding environment by converting sunlight into heat energy. These solar collectors account for approximately 35% of the overall cost of solar cooling systems. Therefore, it is crucial to select an appropriate design and setting for the collector while considering its compatibility and integration with the rest of the solar cooling system [16]. An experimental assessment of the addition of a serpentine tube collector with three different cross-sections showed that the addition of a cooling tube increased the electrical efficiency by almost 12% and provided an additional 22.6 W of thermal power. However, changing the cooling tube configuration from circular to rectangular reduced the electrical efficiency by 2%. Fins in collector tubes passively increase the convection heat transfer rate. These devices, such as twisted tapes, fins, coils, cables, and spirally grooved tubes, create intense mixing between the near-wall and mainstream flows, reduce the thickness of the thermal boundary layer, and increase the tangential velocity. These techniques increase the thermal efficiency of the system, reduce absorbent tube losses, and improve the overall reliability [17].

In addition, adding nanoparticles to purified water as a coolant increases the overall energy and exergy efficiencies by 6.6% and 0.7%, respectively [17]. Increasing the mass flow rate also shows a positive trend in PV performance with collectors in terms of energy efficiency and exergy [18]. The choice of a suitable fluid depends on the operating conditions of the application and the design characteristics. Ideally, the fluid should exhibit good thermal stability, safe operation throughout the desired temperature range, good chemical compatibility with the tube wall material, low cost, and environmental friendliness [19]. A high thermal conductivity, heat capacity, and heat transfer coefficient are desirable for maximizing heat transfer effectiveness [20]. Nanofluids, which are dispersions of nanometer-sized solid particles in a fluid, increase the thermal conductivity, resulting in increased heat transfer [21, 22]. Nanofluids that are commonly used as solar panel coolants include Cu, Al_2O_3, and TiO_2. An experimental investigation in Jordan found that electrical efficiency increases with increasing mass flow rate from 0.5 kg/min to 5 kg/min, and Al2O3 nanofluids give better electrical results than TiO_2 [23].

The potential for enhancing PV solar cell efficiency lies in modifying the collector of the cooling system by incorporating a collector that employs a nanofluid as a medium. Research has explored alterations in collector design, revealing that changes can influence performance through the expansion of the heat transfer surface area. Additionally, the introduction of fins into the collector has been observed to impact the rate of convective heat transfer within the system [24, 25]. Performance also increased with working fluids and flow rates with high thermal conductivity. Therefore, we conducted a computational fluid dynamics (CFD) study on collector engineering in PV solar cell cooling systems [22, 26, 27]. CFD modeling with ANSYS enables the examination of temperature reduction in PV solar cells using a thermal collector. Simulations are employed to investigate the utilization of collectors with complex geometries, cost reduction, and mitigation of the risk of errors in future research. [28, 29].

Several studies have shown that cross-sectional area has a significant effect on the rate of heat transfer. In addition, nanofluids have become a topic of active research as working fluids in heat-exchange systems. Therefore, this study aims to identify the collector shape and fins required to increase the contact area by utilizing nanofluid at specific concentrations. Analysis was conducted using ANSYS software to investigate the heat transfer phenomena within the collector and solar panels. The mass flow rates were varied to determine the efficiency of the proposed system and to aid in the development of an improved PVT (photovoltaic thermal) system.

2. Development And Application System

PVT collectors are hybrid systems that combine traditional PV solar cells with thermal collectors to generate electricity and heat. The construction process involved selecting high-quality PV cells, designing the thermal component, integrating the absorber plate, and encapsulating and insulating the PVT collector assembly. The PV cells were mounted on the front surface of the collector assembly, facing the sun, and connected in series or parallel to achieve the desired voltage and current output. The fluid connection and circulation system connect the HTF channels to the pumps, heat exchangers, and control mechanisms. The PVT collector was mounted and installed on a suitable structure to ensure proper orientation and tilt angles to maximize solar exposure. Electrical and monitoring systems track the performance of the PVT collector by providing real-time data on electricity generation, heat production, and fluid temperature. Regular maintenance is crucial for the optimal performance and longevity of PVT collectors. Interdisciplinary collaboration among experts in PVs, thermal engineering, materials science, and construction is essential to fabricating an effective and durable hybrid system that efficiently generates electricity and heat [30].

PV thermal (PVT) collectors combine PV solar cells with thermal collectors to create a more efficient and versatile energy system. This hybrid approach offers simultaneous electricity generation and heat collection, thereby increasing overall energy efficiency. The key considerations include material selection, compatibility, design optimization, heat absorber integration, heat transfer fluid (HTF) system development, thermal insulation, electrical and thermal

integration, integration with building structures, efficiency enhancement, monitoring and control systems, lifecycle analysis, research and development, and testing and validation. Collaboration among experts in PVs, solar thermal systems, materials science, and engineering is essential for the successful integration of PVT collectors. By focusing on materials, design optimization, heat absorption, heat transfer fluids, thermal insulation, electrical and thermal integration, and lifecycle analysis, PVT collectors can contribute to more sustainable and energy-efficient solutions for power generation and thermal applications [31].

PVT collectors are versatile hybrid systems that combine PV solar cells with thermal collectors and offer numerous benefits across various sectors. They can be integrated into residential and commercial buildings, industrial processes, district heating and cooling systems, agriculture and greenhouses, off-grid applications, solar cooling and air-conditioning systems, hybrid electric vehicles, renewable energy integration, urban infrastructure, research and educational facilities, emergency and disaster relief efforts, and wastewater treatment plants. These systems generate electricity and thermal energy, improve energy efficiency, reduce utility bills, and improve overall energy efficiency. The application of PVT collectors varies depending on factors such as climate, energy requirements, available space, and economic considerations. Overall, integrating PV solar cells with thermal collectors offers a multifunctional solution that enhances energy efficiency and contributes to sustainable development across various sectors.

3. System Model Description

Figure 1 illustrates the cooling of PV solar cells by placing a thermal collector underneath them. The fluid flow of the thermal collector was used for cooling. The power of a water pump was used to move the fluid. The temperature of the cooling fluid increases with time. The capacity of the cooling fluid to absorb heat increases as its temperature rises, resulting in a decrease in the solar cell temperature and an increase in the performance and efficiency of the PV solar cell. A system that uses a PV solar cell cooling technique generates both electrical and thermal energy [22, 32].

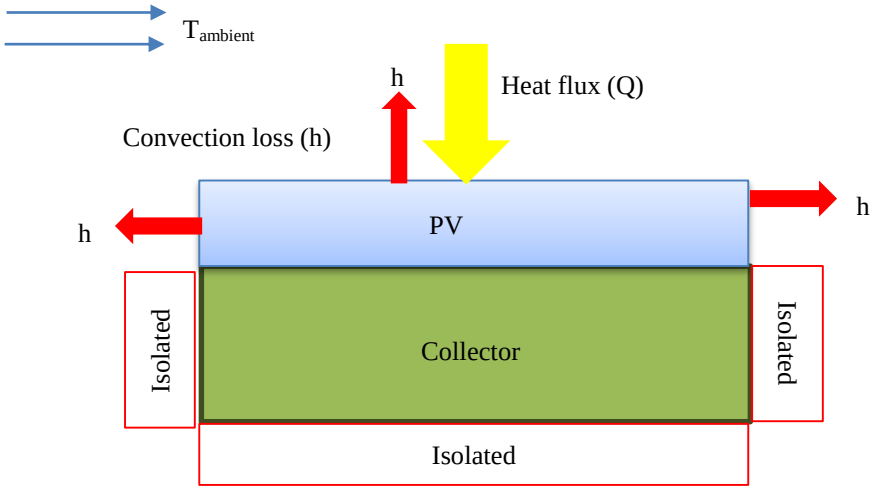

Figure 1. Schematic of a PV solar cell cooling system using a thermal collector

The study's model material used a PV solar cell module with dimensions of 660 × 540 × 4.33 mm and a temperature coefficient of -0.4%/K. The design structure shows the PV geometric design. Table 1 lists the designs and characteristics of the solar cells. Figure 2-b illustrates the design of a thermal collector using direct flow.

Table 1. Coating specifications for PV solar cells with thermal collector cooling [33]

Layers	Density (kg/m^3)	Specific heat capacity (J/kgK)	Thermal conductivity (W/mK)	Thickness (mm)
Glass	2450	790	0.700	3,20
EVAs	960	2090	0.311	0.50
PV cells	2330	677	130	0.21
EVAs	960	2090	0.311	0.50
PVF	1200	1250	0.150	0.30
Collectors	2719	871	202,400	1

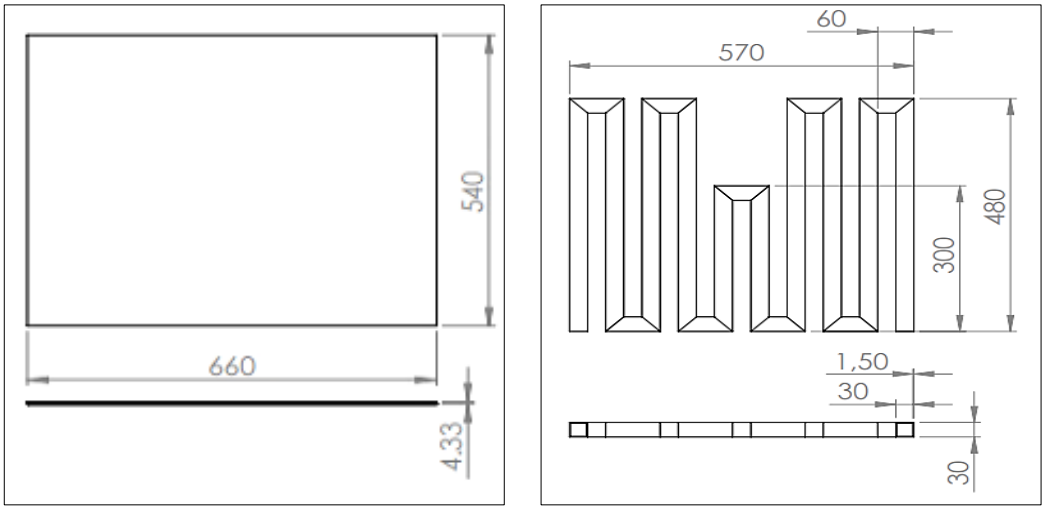

(a) (b)

Figure 2. Geometry (a) PV solar cell (b) thermal collector (unit: mm)

Several researchers have attempted to identify an ideal collector design for PV solar cell cooling to achieve the highest electrical efficiency. A previously published research collector design was modified for this study. As illustrated in Figure 3-a, the collector has a straight-flow design with input dimensions of 30 × 30 mm. In this study, the collector design was changed by adding fins. Aluminum was used as the collector material, and the pipe thickness in the simulation was 1 mm. Figure 3-b illustrates the finned collector design.

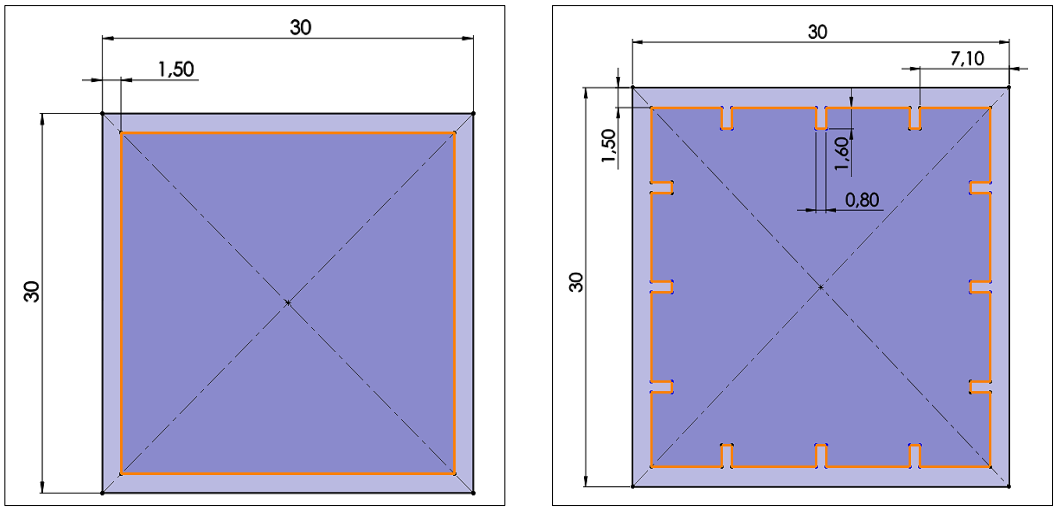

(a) (b)

Figure 3. Thermal collector input geometry (a) Without 0S-Fin (b) 12S-Finned (unit: mm)

The mixing of working fluids was made more efficient and effective by the addition of nanoparticles. In particular, mixing can increase the thermal conductivity, increase convection heat transfer, and decrease thermal losses. In addition, the nanoparticle content of the base fluid contributes to a considerable reduction in the effective thermal stress on the collector [34]. The high thermal conductivity of Al_2O_3 makes it interesting to investigate [35]. The properties of the Al_2O_3 nanofluid and water as the primary working fluid are listed in Table 2.

Table 2. Characteristics of the Concentration of Water/ Al_2O_3 [35]

Concentration Water/Al_2O_3	density, ρ (kg/m^3)	Specific heat, c (J/kgk) c_p	Thermal conductivity, k (W/mK)	Viscosity, μ (kg/ms)
φ = 0%	998,2	4182,0	0.600	0.001003
φ = 1%	1007,4	4194.7	0.765	0.000612
φ = 3%	1059,8	4086,2	0.798	0.000642
φ = 5%	1112,2	4017,8	0.828	0.000672

The following assumptions and elements were used to simplify the numerical modeling: the collector is perfectly isolated. Very little PV radiation is lost. The system does not have an energy generator. In the fluid flow under steady-state circumstances, the PV system alone experiences convection losses, and all heat transmissions occur. The area surrounding the system was maintained at a constant ambient temperature. The thermophysical characteristics of each solid layer of a solar device are believed to have fixed values. The simulation's highest temperature was utilized to calculate the PV solar cell efficiency for each modification; convection, thermal conductivity, and specific heat are all examples of thermal characteristics tested in this study. The mass flow rate, viscosity, and other kinematic characteristics of a straight-through collector indicate that turbulent flow occurs at the interface of the collector area with the PV cell [22, 26].

4. System Equations

In this study, the fluid flow and heat transfer within the collector were simulated primarily through the application of continuity, momentum, and energy equations. In addition, various assumptions were incorporated into the analysis, including the incompressibility of the working fluid. Moreover, when calculating the absorption power, it is assumed that the PV cell absorbs the entire incoming heat flux because the only type of heat loss from the panels is stationary convection loss. Hence, the three governing equations in this research are the mass Equation 1, momentum Equation 2, and energy Equation 3 [36].

$$\nabla\left(\rho_{nf}\mu_{nf}\right) = 0 \tag{1}$$

$$\nabla\left(\rho_{nf}\mu_{nf}\mu_{nf}\right) = -\nabla p + \nabla\tau + \rho_{nf}g \tag{2}$$

$$\nabla\left(\rho_{nf}\mu_{nf}C_{p,nf}T\right) = \nabla(k_{nf}\nabla T) \tag{3}$$

where the parameters include the nanofluid's density (ρ_{nf}), viscosity (μ_{nf}), thermal conductivity (k_{nf}), and specific heat ($C_{p,nf}$), PV solar cell temperature (T) and pressure (p). The numerical solutions of the aforementioned equations were used in a three-dimensional computational fluid dynamics model to estimate the temperature distribution of the PV cell and water collector. In the PV cell, only the top surface was exposed to heat flow. Therefore, heat transfer and wind were assumed to exist only in the topmost layer of the PV cell. The external temperature was maintained constant throughout the simulation. The boundary condition for the water inlet was set at an absolute pressure, and the conditions for the water inflow and outflow were identical. In other words, during the simulation, environmental parameters such as the external temperature, inlet water pressure, and water conditions at the inflow and outflow were maintained constant according to predefined parameters.

When solar radiation is absorbed, the operating temperature of PV solar cells increases significantly, which is inversely related to their electrical efficiency. Equation 4 describes how to represent electrical efficiency (η_{el}) [37].

$$\eta_{el} = \eta_{ref}[1 - \beta_{ref}\left(T_c - T_{ref}\right)] \tag{4}$$

CFD simulations were performed to determine the PV's ultimate average temperature and to compute the magnitude of η_{el} using Equation 4, where β_{ref} is the temperature coefficient of the PV solar cell, η_{ref} is the PV solar cell reference efficiency, and Tref is the PV starting reference temperature. For silicon-based PV solar cells, the η_{ref} and β_{ref} are 0.12% and 0.0045/℃, respectively, when the T_{ref} is 25 ℃. Meanwhile, equation 5 may be used to get the thermal efficiency (η_{th}) [22].

$$\eta_{th} = \frac{mc_p(T_o - T_i)}{QA} \tag{5}$$

where T_0 is the output temperature generated by the fluid CFD simulation, C_p is the specific heat capacity of the heat transfer fluid, and m is the mass flow rate. T_i is the initial temperature of the incoming fluid collector; A is the collector cross-sectional area and Q represents the solar irradiation intensity/heat flux value.

In this study, statistical analysis was employed to gain insight into the relationships between the variables. Specifically, we utilized a two-way analysis of variance (ANOVA) without replication to investigate how changes in the means of the quantitative variables were influenced by the values of the two categorical variables. ANOVA was used to determine whether there were significant differences between two or more groups or treatments within a single analysis. This helps identify the effect of independent variables on the dependent variable [38]. ANOVA can provide information about the statistical significance of differences between groups. ANOVA was performed after the simulations were validated, as shown in Figure 4.

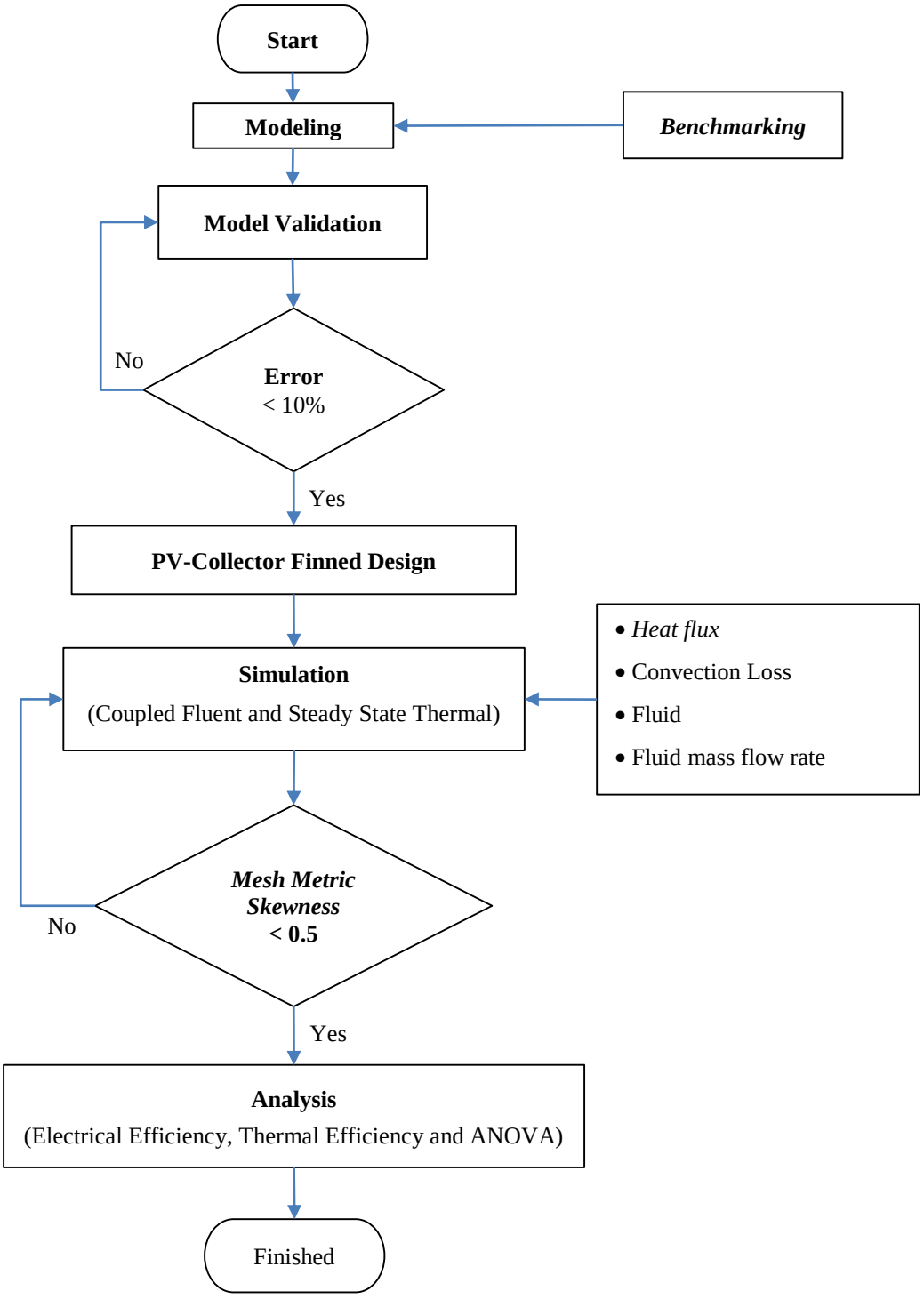

Figure 4. Research flowchart

ANOVA can help researchers draw stronger conclusions about whether the differences are real or merely the result of random variation. This analytical approach allowed us to assess the interactions between the two independent variables and the dependent variable. A significance level of 0.05 was chosen to determine the statistical significance of our findings in the research [39].

5. Computational Fluid Dynamics Study Procedure

The most recent method for examining the performance of PV solar cells with added thermal collectors involves modeling and simulation using a coupled ANSYS system. To enable the development of all the PV layers, as in Arifin's study on PV cooling with heat sinks (2020), the simulation uses only one layer of PV cells [40]. A more significant fluid mass flow is linked to improved electrical and thermal efficiency, according to Rosli's study from 2018, which also reports on this topic [27].

The development process involved modeling PV solar cells by designing the fluid input, mass flow rate, and collector. Fins can be added to thermal collectors to improve collector engineering. Water and Al_2O_3 nanofluids at varying concentrations were used as the flowing fluids. The total mass flow rates in the reference studies were 0.03, 0.05, 0.07, and 0.09 kg/s.

The k-ε re-normalization group (RNG) turbulence model and steady-state simulations were both employed by the ANSYS Fluent program. With a temperature of 28 °C, a turbulence intensity of 5%, and a hydraulic diameter of 0.027 m, the mass flow rate of the input fluid was modified. The coupled Green–Gauss cell-based settlement technique was employed. The set convergent criteria were 10^{-4} for the pressure, velocity, and continuity equations and 10^{-6} for energy [22].

By contrast, the ANSYS Steady-State Thermal program employs a steady-state simulation. Using a heat flux (Q) module, solar radiation of 1000 W/m^2 was modeled. The PV cell surface receives solar radiation in a controlled direction, whereas convection losses affect the surfaces of the other domains. On the entire surface of the PV solar cell, at 10 W/m^2°C, it is expected that little heat transfer or convection losses (h) take place. A solid-interface fluid was applied to the PV surface. The boundary conditions employed in the CFD simulations are shown in Figure 5.

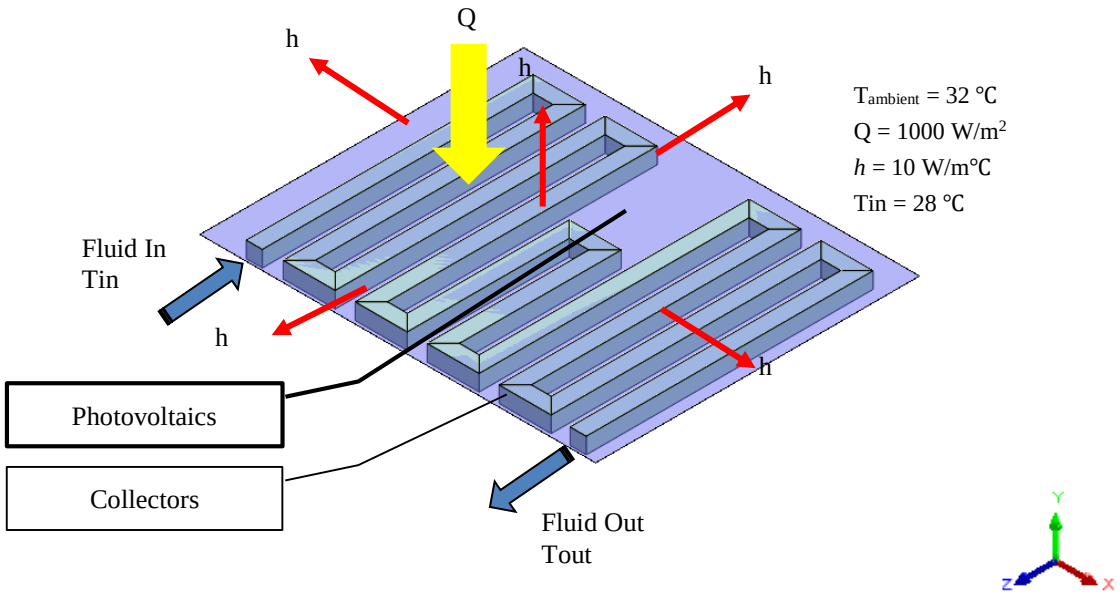

Figure 5. System boundary conditions in this study

The quality of the mesh determines the accuracy of the simulation. More precise findings are obtained with more minor, denser webs, while more extended simulation periods and an excessive number of meshes may degrade computer performance [41, 42]. The default mesh design was employed, with the curvature determined by the global metric and the fineness of the mesh level adjusted to fine. By default, the PV geometry utilizes a mesh, whereas the collector geometry employs proximity. Mesh independence testing was performed to determine the ideal mesh size for a specific shape. Mesh testing was performed using a radiation dose of 1000 W/m^2 and a mass flow rate of 0.09 kg/s. Mesh variation was accomplished by altering the mesh body size, which ranged from 3 mm to 11 mm.

6. Computational Fluid Dynamics Study Procedure Validation

To ensure that the simulation results based on the research produced the same outcome values, a validation was carried out. This was demonstrated by equating the system temperature distribution data using a benchmark research model. The validation criteria were based on an error value of less than 10% when the study findings were compared with the reference research. Based on the study conducted by Rosli (2018), this research was validated in a CFD study [27].

Figure 6 shows the results of the simulation and the reference research. Based on the trend generated for each fluid mass flow rate to the PV temperature, the study results exhibited the same trend as the reference study. The U-Flow collector had the lowest temperature for research studies as well as for reference research. There is no significant gap in the research studies conducted with reference research, where the lowest PV temperature was produced using the U-Flow collector and the highest PV temperature was produced using the serpentine collector for each fluid mass flow rate.

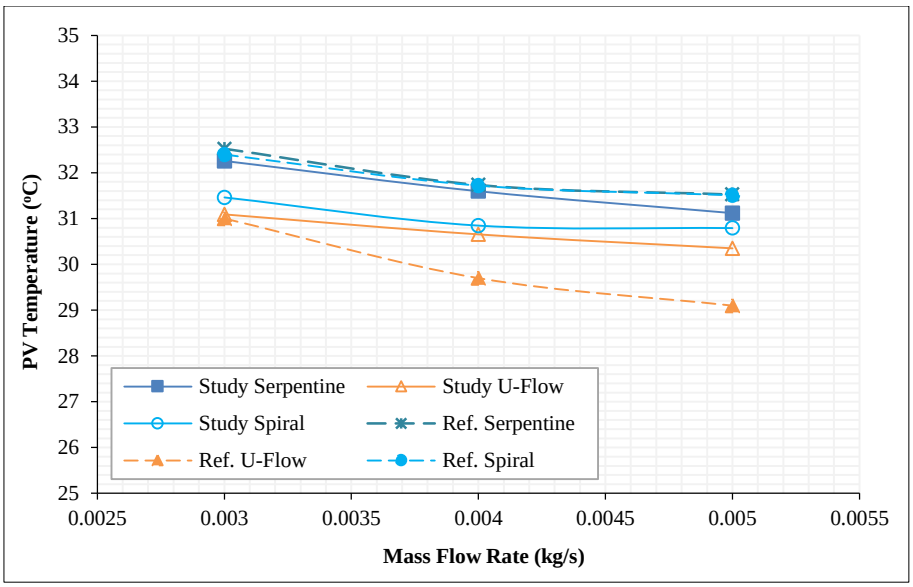

Figure 6. Changes in PV temperature for each mass flow rate based on the reference study

The contours produced in the research studies have a contour shape that resembles the results of the reference study in the temperature range of 300 K to 307 K, as shown in Figure 7. Serpentine collectors have a red contour in research studies and reference study, where the red contour indicates high-temperature solar cell PV. Meanwhile, the lower the PV cell temperature, the more dominant the blue contour color. The dominant blue contour in the PV solar cells was found in collectors with a U-shape in this study and the reference study results. This indicates that the color contours resulting from the research studies have values close to those of the reference research.

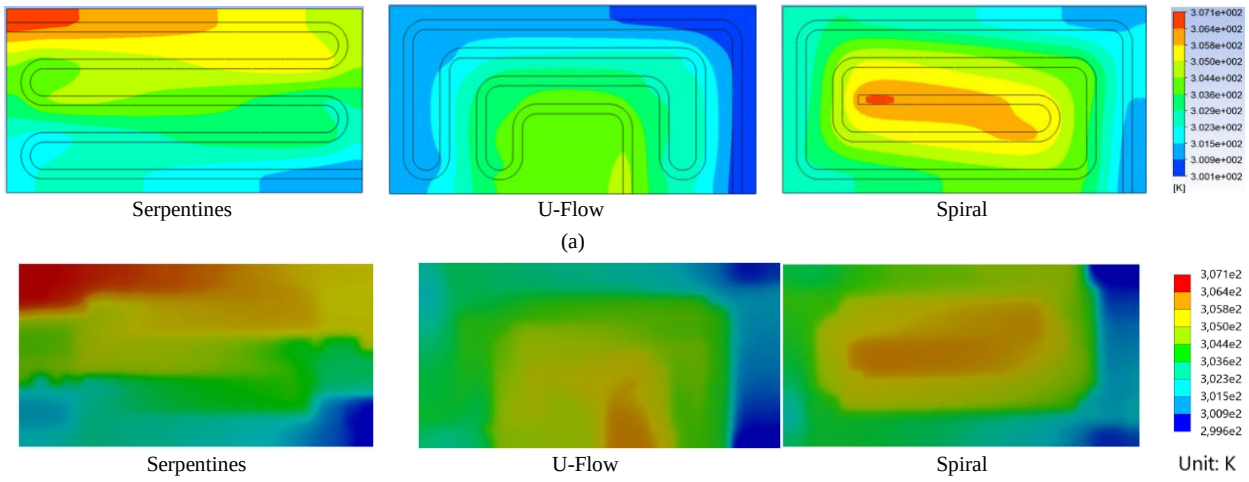

Figure 7. Contour PV temperature simulation results (a) Rosli et al. (2018) [27] (b) Reference study

The difference in the percentage error of the PV temperature between the simulation results of this study and those of the reference research simulations varied between 0.3% and 4.3%, as listed in Table 3. The largest error difference was 4.3% when the U-flow collector was used at a fluid mass flow rate of 0.005 kg/s. Therefore, the method used in this study has a valid value and is assumed to be applicable to the cases in this study.

Table 3. Percentage of error PV temperature research validation

Design	Mass flow rate (kg/s)		
	0.003	**0.004**	**0.005**
Serpentines	0.8%	0.4%	1.3%
U-Flow	0.3%	3.2%	4.3%
Spiral	2.9%	2.7%	2.3%

7. Results and Discussion

The characteristics affecting the cooling of PV solar cells using a thermal collector were successfully determined by CFD modeling and simulation. The design of the collector with fins, fluid mass flow rate, and nanofluid water/Al_2O_3 was examined for each primary working fluid concentration. The optimization simulation was performed using ANSYS Fluent and Steady-State Thermal 18.2. The findings of the optimized simulation are discussed in this section. All energy exchanges with the thermal collector and the PV solar cell efficiency (both electrical and thermal efficiency) were estimated after CFD modeling using the comprehensive ANSYS software for all parameters. Based on these results, the effect of each factor was observed using ANOVA.

7.1. Temperature Simulation Results

Simulations were successfully performed using ANSYS Steady-State Thermal on PV solar cells for a radiation intensity or heat flux of 1000 W/m^2 with a natural convection of 10 W/m^2℃ and an ambient temperature of 32 ℃. The thermal collector system was coupled using ANSYS Fluent with working fluid Al_2O_3 nanofluid (0%, 1%, 3%, and 5%) and mass flow rates (0.03, 0.05, 0.07, and 0.09 kg/s). An input temperature of 28 ℃ was input for the fluid as a riser collector configuration without fins (0S) and with collector fins (12S). The final PV temperature and fluid output were generated for electrical and thermal efficiency analyses.

The temperature of the PV solar cell decreased when an Al_2O_3 nanofluid was used on a 12S-finned collector, as shown in Figure 8. In addition, increasing the mass flow rate of the fluid decreased the temperature of the PV solar cell. The addition of fins to the thermal collector widened the heat transfer area between the thermal collector and the working fluid. By adding nanoparticles in the form of Al_2O_3, the working fluid changes its characteristics by increasing its specific heat. Increasing the mass flow rate of the fluid accelerated the heat exchange in the working fluid. The lowest PV solar cell temperature, 29.654 ℃, was generated using a 12S-finned thermal collector system with 1% water/Al_2O_3 nanofluid at a mass flow rate of 0.09 kg/s.

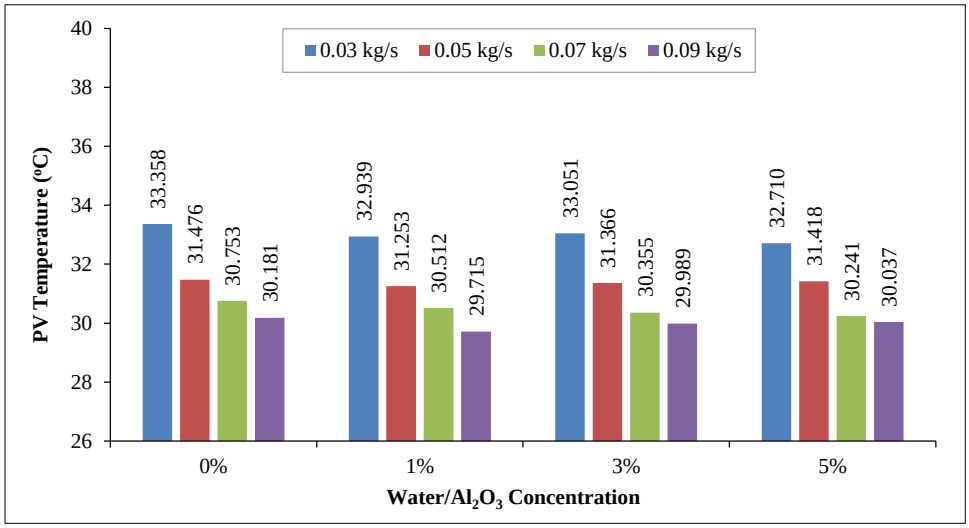

(a)

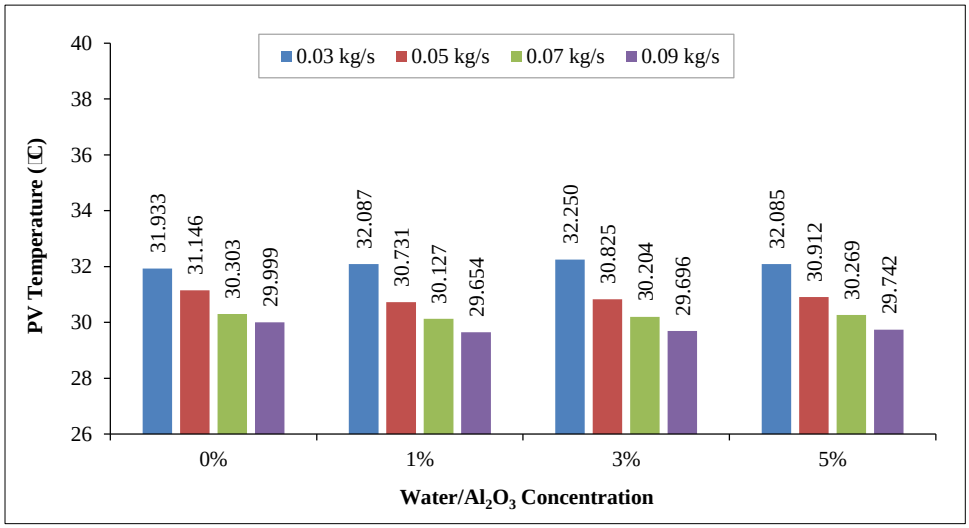

(b)

Figure 8. PV temperature at different mass flow rates and nanofluid concentrations for each PV using a collector (a) with fins-0S and (b) without fins-12S

The fluid output temperature can be reduced by adding the self to the thermal collector, increasing the mass flow rate of the fluid, or adding a mass fraction to the Al_2O_3 nanofluid, as shown in Figure 9. The use of fins in the collector affects the fluid flow path to the collector, thereby affecting the fluid output temperature. With a stable fluid input temperature, the addition of a nanofluid weight fraction can increase the specific heat of PV solar cells during heat transfer. In addition, increasing the fluid mass flow rate significantly affected the output temperature of the fluid. The lowest fluid output temperature (29.994 ℃) was also generated in a system that uses a 12S-finned thermal collector with 1% water/Al_2O_3 nanofluid at a mass flow rate of 0.09 kg/s.

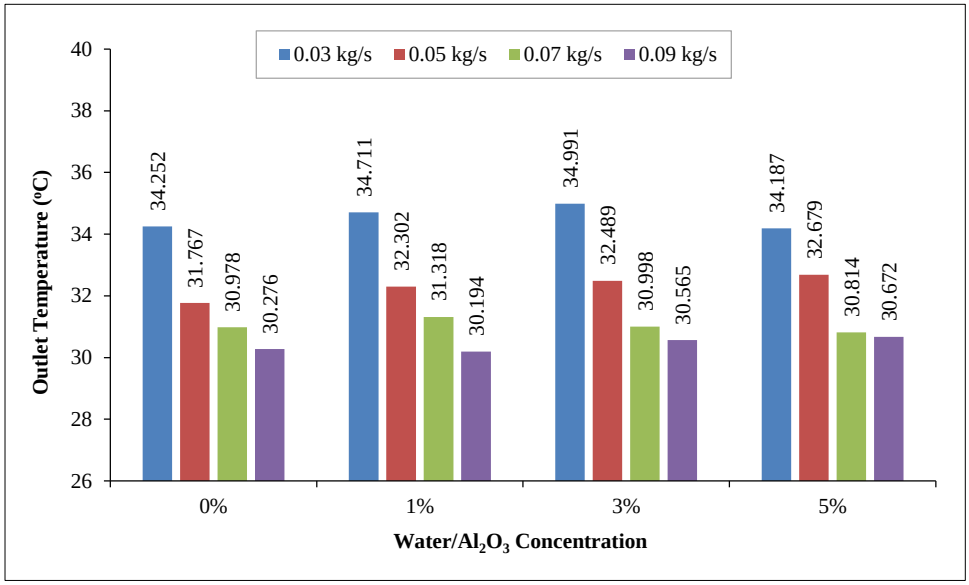

(a)

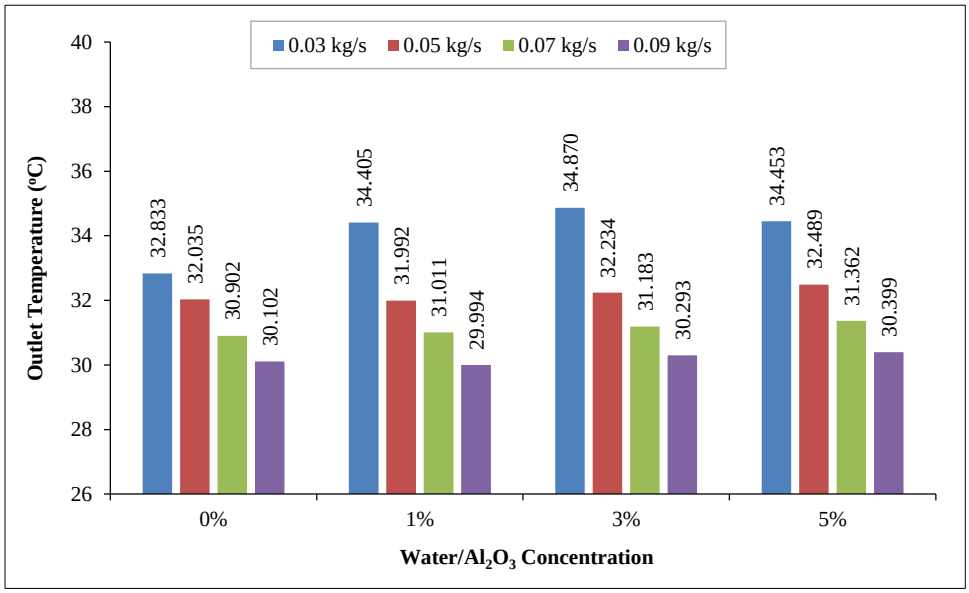

(b)

Figure 9. Fluid output temperature at different mass flow rates and nanofluid concentration for each PV using a collector (a) with fins-0S (b) without fins-12S

A mesh independence test was performed to optimize the computational accuracy and process of the modeling simulation. This test was conducted on the system that produced the lowest PV temperature and output fluid. The system using a 12S-finned thermal collector with 1% water/Al_2O_3 nanofluid at a mass flow rate of 0.09 kg/s was investigated while the other boundary conditions remained the same. The meshing process was varied with different mesh body sizes (3, 5, 7, and 11 mm) with the other mesh boundary conditions remaining constant. As shown in Figure 10, the temperature results for the PV solar cell and fluid output for each mesh body size exhibited similar trends. The difference between the minimum and maximum values generated in the mesh-independence process had an error value of 2.51%. The mesh body size of 5 mm had nodes and mesh elements 47325 and 226234, with an average skewness value of 0.25. Therefore, the mesh was of good quality and produced accurate simulations.

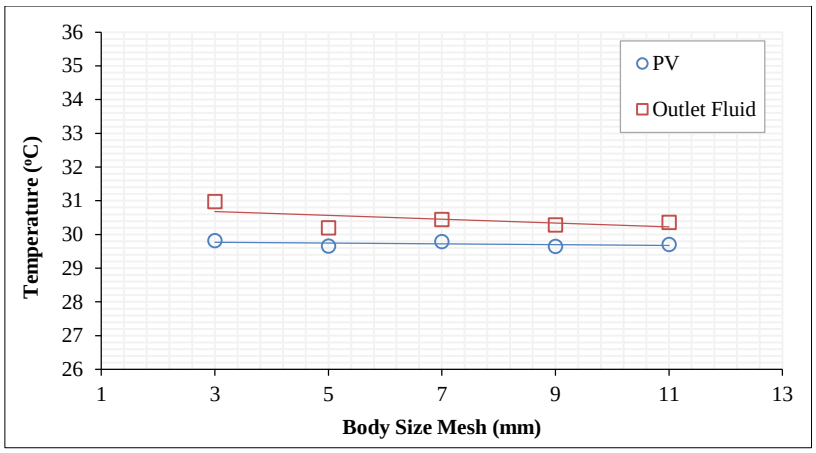

Figure 10. Independence of simulation study mesh

7.2. Simulation Result Temperature Contour

Figure 11 shows the difference in temperature distribution in PV solar cell systems using a thermal collector without fin (0S) and with fins (12S). The temperature distribution of the PV solar cells had color contours that were similar to those with and without fins, with a temperature range of 27.4 to 33 ℃. The contour distribution of the PV solar cells using the 12S-finned thermal collector was smoother and did not break. This is due to the broader and faster absorption of heat, marked by the distribution of the collector fluid contours, which have more dominant green contours on the fluid side after entering the collector. In addition, the use of fins on the collector affects the direction of fluid flow in the absorption and heat transfer processes. Different fluid-flow directions were identified based on the temperature distribution at the fluid output. The temperature distribution at the output of the fluid with thermal collector fins has a color contour that is less regular than that of the thermal collector without fins.

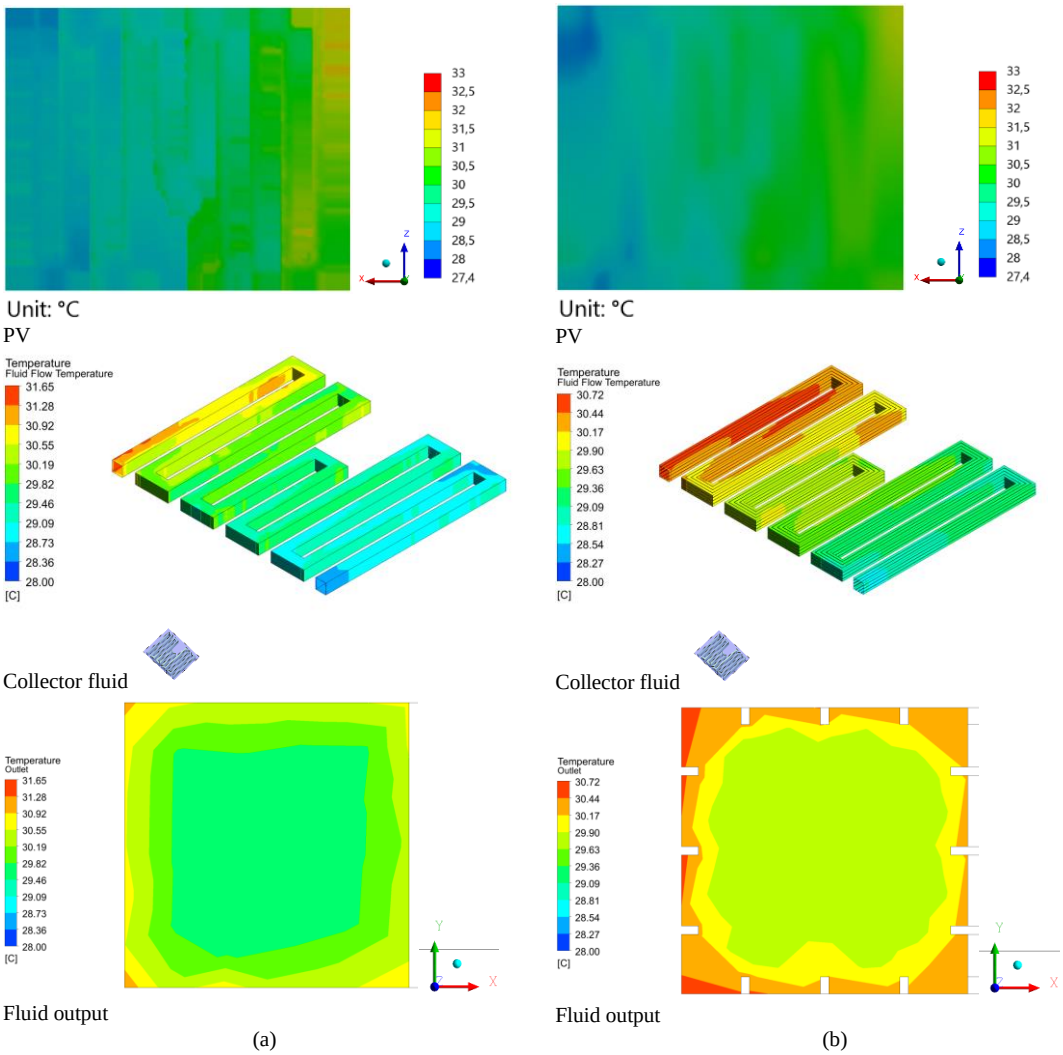

(a) (b)

Figure 11. Temperature distribution of PV solar cell systems using thermal collectors (a) without fins (0S) (b) 12S-finned

In a PV solar cell system with a thermal collector, the mass flow rate of the fluid is vital for reducing the temperature of the PV solar cell. As shown in Figure 12, the temperature distribution of the PV solar cell has a different color contour for each increasing fluid mass flow rate. The contour distribution of the PV solar cell temperature was obtained from the simulation results using a 12S-finned collector with a working fluid of 1% water/Al_2O_3 nanofluid. The temperature distribution of the resulting PV solar cells was in the range of 27 to 38℃. Based on the figure, the highest fluid mass flow rate, which is 0.09 kg/s, has a blue color contour that is more dominant than the others, with no yellow or red contour. The dominant blue contour indicates the low temperatures of the PV solar cells.

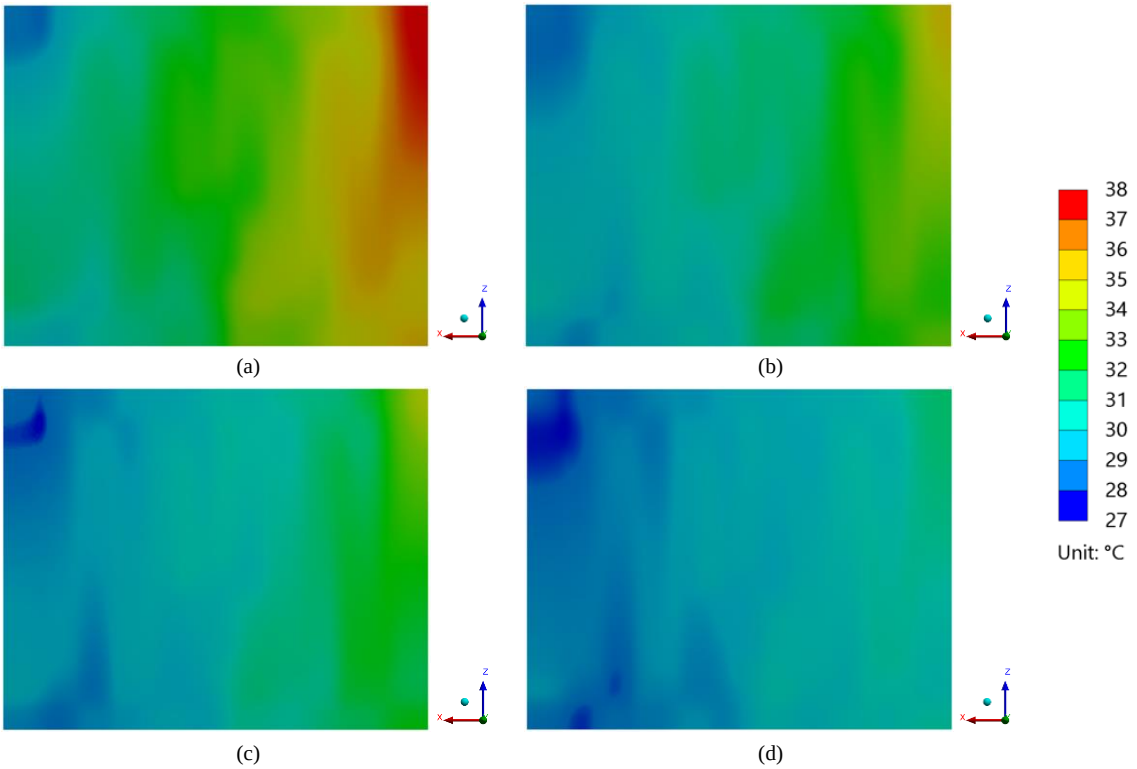

Figure 12. PV solar cell temperature distribution for each fluid mass flow rate (a) 0.03 kg/s (b) 0.05 kg/s (c) 0.07 kg/s (d) 0.09 kg/s

Using water/Al_2O_3 nanofluid as a working fluid produces a distribution of color contours at different temperatures, as shown in Figure 13. The color contours of the PV solar cells using a 12S-finned thermal collector at a fluid mass flow rate of 0.09 kg/s were obtained. The temperature distribution of the resulting PV solar cells ranged from 28.5 to 33 □C. It can be seen that the 1% water/Al_2O_3 working fluid has more dominant blue and green contours. In addition, there was no yellow or red contour, which indicate high temperatures. The temperature distribution of PV solar cells with a working fluid of 1% water/Al_2O_3 had better specific heat than the other working fluids.

7.3. Performance of PV Solar Cells Using a Thermal Collector

The effectiveness of the generated power provides insight into the functioning of the PV solar cells. Compared with water-based fluids, the use of Al_2O_3 nanofluids at various concentrations affects the fluid production and temperature variations in PV solar cells. Consequently, the electrical and thermal efficiencies are different. The resultant temperature differential from the reference temperature provides insight into electrical efficiency. Simultaneously, the specific heat of the fluid has a significant impact on thermal efficiency.

The nominal reference efficiency was 0.12 with a temperature coefficient of 0.0045 /℃ at a reference temperature of 32 ℃. As shown in Figure 14, the use of a 12S-finned thermal collector and water/Al_2O_3 as a working fluid can increase the electrical efficiency of the PV solar cell owing to the decrease in the temperature of the PV solar cell. In addition, the electrical efficiency increased with the mass flow rate of the fluid. As with the lowest PV solar cell temperature value, in the 12S-finned thermal collector system with 1% water/Al_2O_3 nanofluid at a mass flow rate of 0.09 kg/s, the system produces the highest electrical efficiency of 11.749%. The lower the temperature of the PV solar cell, the higher the electrical efficiency, which approaches the reference efficiency.

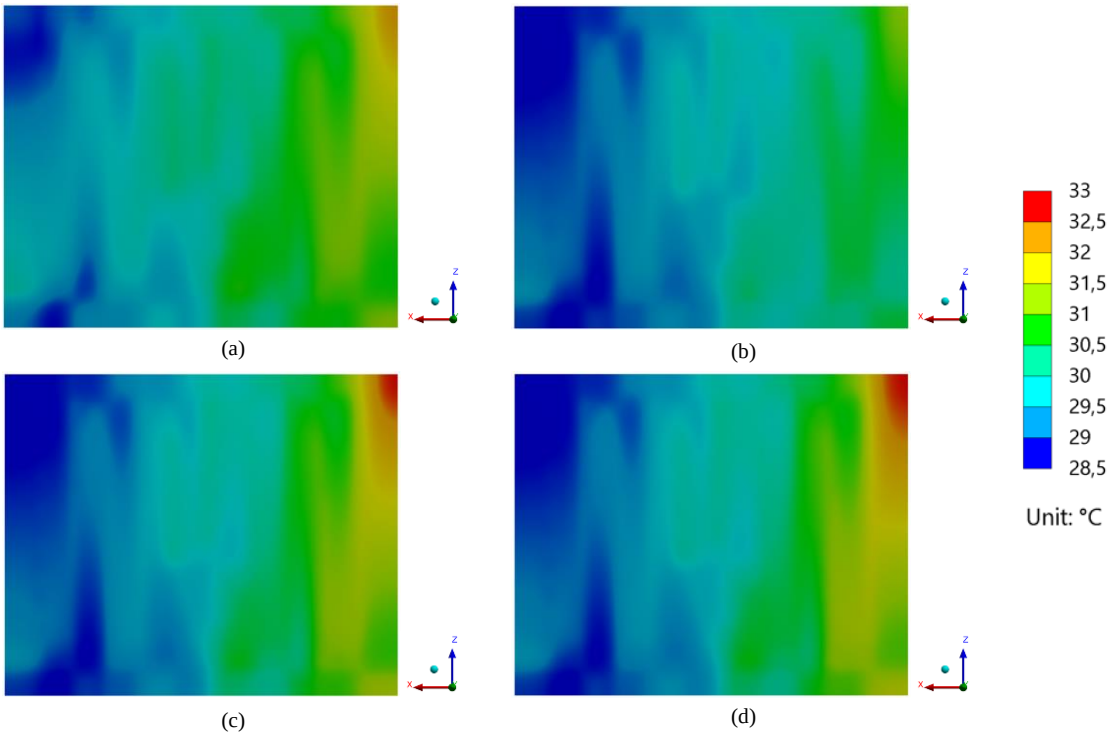

Figure 13. PV solar cell temperature distribution for each working fluid water/Al_2O_3 (a) 0% (b) 1% (c) 3% (d) 5%

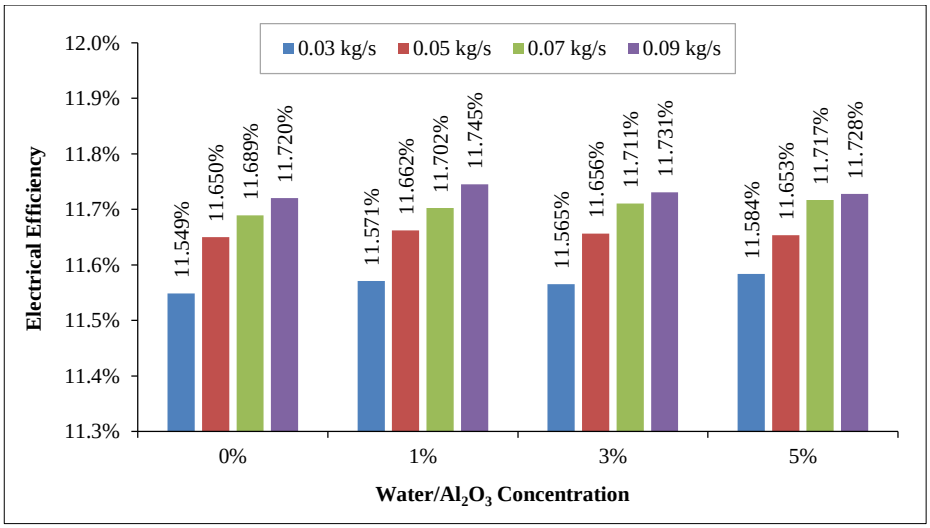

(a)

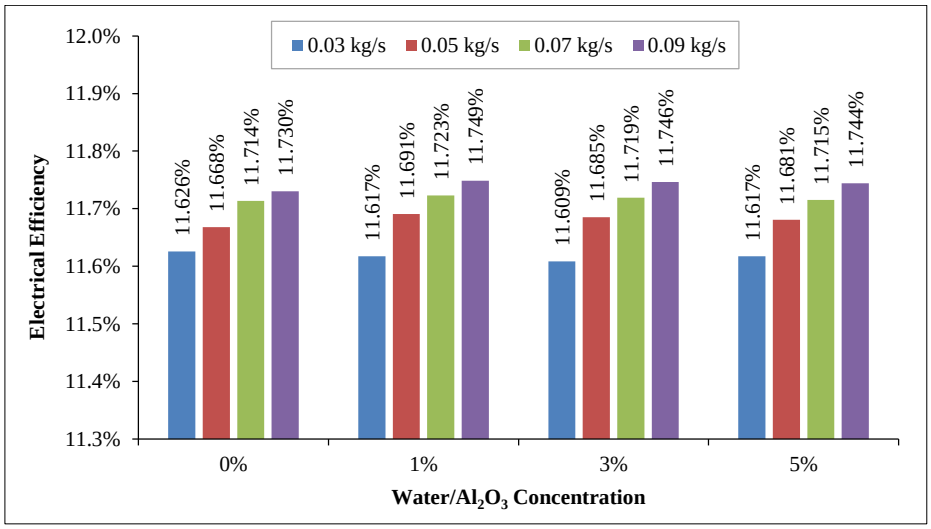

(b)

Figure 14. Electrical efficiency and PV temperature of different mass flow rates and nanofluid concentrations for each PV using collectors (a) without fins (0S) (b) with fins (12S)

The resulting thermal efficiency is one of the advantages of using a thermal collector system to cool PV solar cells. It can be seen that the thermal efficiency is affected by the specific heat of the working fluid, water/Al_2O_3, and the output temperature of the resulting fluid. As shown in Figure 15, the thermal efficiency increased after using a 12S-finned thermal collector system with water/Al_2O_3 nanofluid. The highest thermal efficiency was 68.796% in the 12S-finned collector system using 5% water/Al_2O_3 when the mass flow rate of the fluid was 0.09 kg/s.

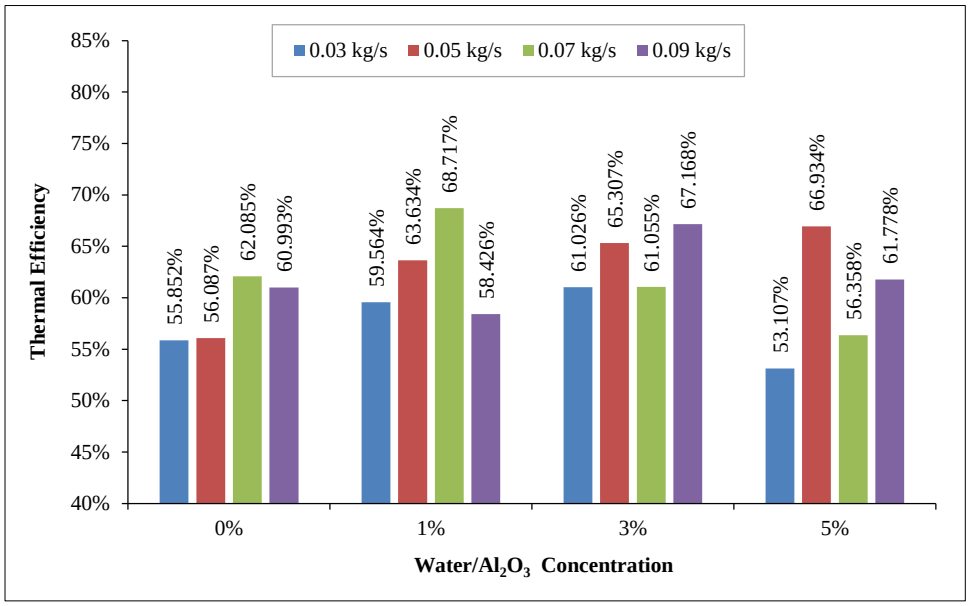

(a)

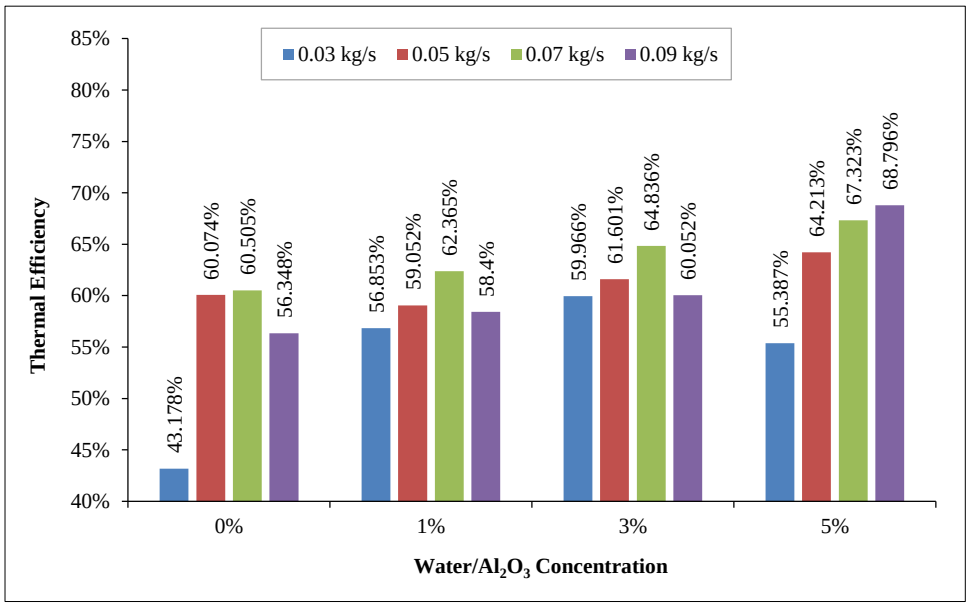

(b)

Figure 15. Thermal efficiency of PV temperature on different mass flow rates and nanofluid concentrations for each PV using (a) 0S-finned and (b) 12S-finned collectors

7.4. The Effect of Fluid Mass Flow Rate and Al2O3 Nanofluid Concentration on the Electrical Efficiency of PV Solar Cells

Based on the generated electrical efficiency data for each mass flow rate and nanofluid concentration variation in the system, the results were grouped in Table 4. The data were grouped to determine the effect of system variations and their relationship with the increase in the performance of the PV solar cells based on the generated electricity efficiency. The analysis was performed using a two-way ANOVA method without replication, with a significance value of 0.05. The p-value of the mass flow rate was 7.98E-09; therefore, the mass flow rate affected the efficiency of the generated electricity. Simultaneously, the Al_2O_3 fluid concentration had no effect on the electrical efficiency because the P value was 0.293. Additionally, 1.18E-06, as shown in Table 5.

Table 4. PV solar cell electrical efficiency data for each fluid mass flow rate and water/ Al_2O_3 nanofluid concentration

SUMMARY	Count	Sum	Average	Variances
0.03kg/s	4	0.464688	0.116172	4.89E-09
0.05kg/s	4	0.467248	0.116812	9.21E-09
0.07kg/s	4	0.468712	0.117178	1.76E-09
0.09kg/s	4	0.469691	0.117423	7.01E-09
0%	4	0.467374	0.116844	2.22E-07
1%	4	0.467797	0.116949	3.24E-07
3%	4	0.467594	0.116898	3.56E-07
5%	4	0.467576	0.116894	2.97E-07

Table 5. ANOVA results of PV solar cell electrical efficiency for each fluid mass flow rate and water/Al_2O_3 nanofluid concentration

Source of Variation	SS	df	Ms	F	P-values	F crit
Mass flow rate	3.55E-06	3	1.18E-06	230,315	7.98E-09	3.862548
Al_2O_3 Fluid Concentration	2.23E-08	3	7.44E-09	1.447711	0.292629	3.862548
Error	4.63E-08	9	5.14E-09			
Total	**3.62E-06**	**15**				

7.5. The Effect of Fins on Collector and Concentration of Al_2O_3 Nano Fluid on the Electrical Efficiency of PV Solar Cells

Table 6 shows the PV solar cell electrical efficiency data generated for each collector type and water/Al_2O_3 nanofluid concentration. Data were analyzed using a two-way ANOVA without replication, with a significance value of 0.05. An analysis was conducted to determine the effects of the variables. Table 7 shows that the type of finned collector does not change the response to the Al_2O_3 fluid concentration, and vice versa. This was because the MS error value was smaller than the MS error value for the two variations, which was equal to 1.8E-09. Finned collectors are known to influence the electrical efficiency of PV solar cells, with a P value of 0.033.

Table 6. Electrical efficiency of PV solar cells for each collector type and nanofluid concentration

SUMMARY	Count	Sum	Average	Variances
No Fin-0S	4	0.469242	0.117311	1.11E-08
Finned-12S	4	0.469691	0.117423	7.01E-09
0%	2	0.234503	0.117251	4.83E-09
1%	2	0.234941	0.11747	5.43E-10
3%	2	0.23477	0.117385	1.25E-08
5%	2	0.234719	0.11736	1.27E-08

Table 7. ANOVA results of PV solar cell electrical efficiency for each collector type and nanofluid concentration

Source of Variation	SS	df	Ms	F	P-values	F crit
Collector Type	2.52E-08	1	2.52E-08	13.96813	0.033404	10.12796
Al_2O_3 Fluid Concentration	4.89E-08	3	1.63E-08	9.03711	0.051762	9.276628
Error	5.41E-09	3	1.8E-09			
Total	**7.94E-08**	**7**				

7.6. The Effect of Fins on Collectors and Fluid Mass Flow Rates on the Electrical Efficiency of PV Solar Cells

The interaction between the type of collector and mass flow rate of the fluid on the electrical efficiency of the solar cells was studied using a two-way ANOVA without replication, with a significance value of 0.05. The analysis was performed by grouping the PV solar cell electrical efficiency data for each collector type and fluid mass flow rate, as listed in Table 8. Based on the analysis results in Table 9, the collector type does not interact with the differences in the mass flow rate of the fluid used. This was because the MS error value was 1.19E-08, which was smaller than the MS value for each variation used.

Table 8. PV solar cell electrical efficiency data for each collector type and fluid mass flow rate

SUMMARY	Count	Sum	Average	Variances
No Fin-0S	4	0.466821	0.116705	4.43E-07
Finned-12S	4	0.467576	0.116894	2.97E-07
0.03kg/s	2	0.232011	0.116005	5.7E-08
0.05kg/s	2	0.233342	0.116671	3.73E-08
0.07kg/s	2	0.234325	0.117162	1.14E-10
0.09kg/s	2	0.234719	0.11736	1.27E-08

Table 9. ANOVA results of PV solar cell efficiency for each collector type and fluid mass flow rate

Source of Variation	SS	df	Ms	F	P-values	F crit
Collector Type	7.12E-08	1	7.12E-08	5.961724	0.092363	10.12796
Mass flow rate	2.19E-06	3	7.28E-07	60.95936	0.003464	9.276628
Error	3.58E-08	3	1.19E-08			
Total	**2.29E-06**	**7**				

This study analyzed the electrical efficiency of PV solar cells based on system variations in the mass flow rate and nanofluid concentration of Al_2O_3. The interaction of the electrical efficiencies of the solar cells was studied using a two-way ANOVA without replication. The results showed that the mass flow rate affected the efficiency of the generated electricity, whereas the Al_2O_3 fluid concentration had no effect on efficiency. The type of finned collector does not change the response to the Al_2O_3 fluid concentration, but the finned collectors influence the electrical efficiency of PV solar cells. The collector type did not affect the differences in fluid mass flow rates.

This research is comparable to the experimental research conducted previously by other researchers using nano-water/magnetite fluid in finned collectors to improve the performance of PV solar cells [14]. This improvement is achieved by engineering the expansion of the fluid heat transfer surface and improving the fluid characteristics to accelerate heat transfer. Engineering results in an increase in the performance of solar PV cells while simultaneously improving thermal performance.

Simulation research allows for complex designs, saving time and money during experimental research. In addition, simulation reduced the impact of fatal errors in the experimental research process. After the CFD simulation using ANSYS software was completed for all factors, all energy and efficiency interactions of solar PV cells with thermal collectors (electrical and thermal efficiencies) were calculated. However, the results and analyses of the research using CFD must be validated. Experimental validation of PV solar cell hybrid systems using Al_2O_3 nanofluid-based finned thermal collectors under actual environmental conditions must be conducted.

8. Conclusion

CFD modeling and simulations were conducted to identify the parameters affecting the cooling of PV solar cells using a thermal collector. The factors analyzed included collector design, fluid mass flow rate, and the concentration of Al_2O_3 nanofluid. The results were evaluated using ANOVA to optimize the cooling system and enhance the performance of the solar cells in converting solar energy into electricity. The 12S-finned thermal collector system achieved the lowest PV solar cell temperature at 29.654 ℃. Fins, mass flow rate, and Al_2O_3 nanofluid fraction were adjusted to lower the fluid output temperature. The 12S-finned thermal collector with 1% water/Al_2O_3 nanofluid reached the lowest fluid outlet temperature of 29.994 ℃. The electrical efficiency of the PV solar cells is influenced by the Al_2O_3 nanofluid concentration. The reference efficiency is 0.12, with a temperature coefficient of 0.0045/℃ at 32 ℃. The 12S-finned thermal collector and water/Al_2O_3 working fluid increased electrical efficiency by reducing the cell temperature. The electrical efficiency improved at higher fluid mass flow rates. The 12S-finned thermal collector system with 1% water/ Al_2O_3 nanofluid at 0.09 kg/s achieved the highest electrical efficiency at 11.749%, close to the reference efficiency. The 12S-finned thermal collector system with a water/Al_2O_3 nanofluid achieved the highest thermal efficiency, reaching 68.796% at a flow rate of 5% water/ Al_2O_3 working fluid at 0.09 kg/s.

This study analyzed the electrical efficiency data of various proposed systems, including variations in the mass flow rate and concentration of the Al_2O_3 nanofluid. The results indicate that the efficiency is influenced by the mass flow rate, whereas the concentration of the Al_2O_3 nanofluid does not have a significant impact. The type of finned collector also affects the efficiency, but the collector type does not interact significantly with various variations in fluid mass flow rates and concentrations of Al_2O_3 nanofluid. Thus, the selection of the mass flow rate and collector type can be crucial factors in designing a more efficient system to address the high temperatures in PV solar cells. This study is expected to contribute to the development of hybrid PVT systems related to the trending issues of nanofluid utilization in modern industries.

9. Declarations

9.1. Author Contributions

Conceptualization: S.D.P. and Z.A.; methodology: S.D.P. and Z.A.; validation: A.R.P., E.P.B., and Z.A.; formal analysis: S.D.P. and E.P.B.; investigation: S.D.P.; resources: S.D.P. and A.R.P.; data curation: S.D.P., E.P.B., and A.R.P.; writing—original draft preparation: S.D.P. and E.P.B.; writing—review and editing: E.P.B., A.R.P., and Z.A.; visualization: S.D.P. and A.R.P.; supervision.

9.2. Data Availability Statement

The corresponding author may provide the data described in this research upon request.

9.3. Funding

This research was funded by the Research Activity entitled "Development of an Al_2O_3 Nanofluid-Based Thermal Collector to Improve the Performance of Photovoltaic Solar Cells," following the Contract Letter for Implementation of Research Activities Master Contract Number: 160/E5/PG.02.00. PL/2023 and Derivative Contract Number 1280.1/UN27.22/PT.01.03/2023, and sources of funds from the Ministry of Education, Culture, Research, and Technology under the Doctoral Disk Research scheme for the 2023 Fiscal Year.

9.4. Acknowledgements

The author acknowledges Universitas Sebelas Maret in their support. The Ministry of Research, Technology, and Higher Education of the Republic of Indonesia provided the total funding for this study through a grant from Penelitian Disertasi Doktor with the title "Pengembangan Thermal Collector Berbasis Nanofluida Al_2O_3 untuk Meningkatan Unjuk Kerja Sel Surya Photovoltaic" (research grant number 1280.1/UN27.22/PT.01.03/2023).

9.5. Conflicts of Interest

The authors declare no conflict of interest.

10. References

[1] Badawy, W. A. (2015). A review on solar cells from Si-single crystals to porous materials and Quantum dots. Journal of Advanced Research, 6(2), 123–132. doi:10.1016/j.jare.2013.10.001.

[2] Nurwidiana, N., Sopha, B. M., & Widyaparaga, A. (2021). Modelling photovoltaic system adoption for households: A systematic literature review. Evergreen, 8(1), 69–81. doi:10.5109/4372262.

[3] Radziemska, E. (2003). The effect of temperature on the power drop in crystalline silicon solar cells. Renewable Energy, 28(1), 1–12. doi:10.1016/s0960-1481(02)00015-0.

[4] Rejeb, O., Gaillard, L., Giroux-Julien, S., Ghenai, C., Jemni, A., Bettayeb, M., & Menezo, C. (2020). Novel solar PV/Thermal collector design for the enhancement of thermal and electrical performances. Renewable Energy, 146, 610–627. doi:10.1016/j.renene.2019.06.158.

[5] Abo-Elfadl, S., Hassan, H., & El-Dosoky, M. F. (2020). Energy and exergy assessment of integrating reflectors on thermal energy storage of evacuated tube solar collector-heat pipe system. Solar Energy, 209, 470–484. doi:10.1016/j.solener.2020.09.009.

[6] Braun, R., Haag, M., Stave, J., Abdelnour, N., & Eicker, U. (2020). System design and feasibility of trigeneration systems with hybrid photovoltaic-thermal (PVT) collectors for zero energy office buildings in different climates. Solar Energy, 196, 39–48. doi:10.1016/j.solener.2019.12.005.

[7] Kandeal, A. W., Thakur, A. K., Elkadeem, M. R., Elmorshedy, M. F., Ullah, Z., Sathyamurthy, R., & Sharshir, S. W. (2020). Photovoltaics performance improvement using different cooling methodologies: A state-of-art review. Journal of Cleaner Production, 273, 122772. doi:10.1016/j.jclepro.2020.122772.

[8] Pater, S. (2021). Long-term performance analysis using TRNSYS software of hybrid systems with PV-t. Energies, 14(21), 6921. doi:10.3390/en14216921.

[9] Slimani, M. E. A., Sellami, R., Said, M., & Bouderbal, A. (2021). A Novel Hybrid Photovoltaic/Thermal Bi-Fluid (Air/Water) Solar Collector: An Experimental Investigation. Proceedings of the 4th International Conference on Electrical Engineering and Control Applications, ICEECA 2019, Lecture Notes in Electrical Engineering, 682, Springer, Singapore. doi:10.1007/978-981-15-6403-1_47.

[10] Abdullah, A. L., Misha, S., Tamaldin, N., Rosli, M. A. M., & Sachit, F. A. (2019). Numerical analysis of solar hybrid photovoltaic thermal air collector simulation by ANSYS. CFD Letters, 11(2), 1-11.

[11] Yu, Y., Long, E., Chen, X., & Yang, H. (2019). Testing and modelling an unglazed photovoltaic thermal collector for application in Sichuan Basin. Applied Energy, 242, 931–941. doi:10.1016/j.apenergy.2019.03.114.

[12] Arifin, Z., Prasetyo, S. D., Tjahjana, D. D. D. P., Rachmanto, R. A., Prabowo, A. R., & Alfaiz, N. F. (2022). The application of TiO2 nanofluids in photovoltaic thermal collector systems. Energy Reports, 8, 1371–1380. doi:10.1016/j.egyr.2022.08.070.

[13] Simón-Allué, R., Guedea, I., Villén, R., & Brun, G. (2019). Experimental study of Phase Change Material influence on different models of Photovoltaic-Thermal collectors. Solar Energy, 190, 1–9. doi:10.1016/j.solener.2019.08.005.

[14] Shahsavar, A., Jha, P., Arici, M., & Kefayati, G. (2021). A comparative experimental investigation of energetic and exergetic performances of water/magnetite nanofluid-based photovoltaic/thermal system equipped with finned and unfinned collectors. Energy, 220, 119714. doi:10.1016/j.energy.2020.119714.

[15] Prasetyo, S. D., Arifin, Z., Prabowo, A. R., Budiana, E. P., Rosli, M. A. M., Alfaiz, N. F., & Bangun, W. B. (2023). Optimization of Photovoltaic Thermal Collectors Using Fins: A Review of Strategies for Enhanced Solar Energy Harvesting. Mathematical Modelling of Engineering Problems, 10(4), 1235–1248. doi:10.18280/mmep.100416.

[16] Allouhi, A., Kousksou, T., Jamil, A., Bruel, P., Mourad, Y., & Zeraouli, Y. (2015). Solar driven cooling systems: An updated review. Renewable and Sustainable Energy Reviews, 44, 159–181. doi:10.1016/j.rser.2014.12.014.

[17] Shahsavar, A., Eisapour, M., & Talebizadehsardari, P. (2020). Experimental evaluation of novel photovoltaic/thermal systems using serpentine cooling tubes with different cross-sections of circular, triangular and rectangular. Energy, 208(118409). doi:10.1016/j.energy.2020.118409.

[18] Shahsavar, A. (2021). Experimental evaluation of energy and exergy performance of a nanofluid-based photovoltaic/thermal system equipped with a sheet-and-sinusoidal serpentine tube collector. Journal of Cleaner Production, 287, 125064. doi:10.1016/j.jclepro.2020.125064.

[19] Smaisim, G. F., mohammed, D. B., Abdulhadi, A. M., Uktamov, K. F., Alsultany, F. H., Izzat, S. E., Ansari, M. J., Kzar, H. H., Al-Gazally, M. E., & Kianfar, E. (2022). Nanofluids: properties and applications. Journal of Sol-Gel Science and Technology, 104(1), 1–35. doi:10.1007/s10971-022-05859-0.

[20] Calderón, A., Barreneche, C., Palacios, A., Segarra, M., Prieto, C., Rodriguez- Sanchez, A., & Fernández, A. I. (2019). Review of solid particle materials for heat transfer fluid and thermal energy storage in solar thermal power plants. Energy Storage, 1(4), e63. doi:10.1002/est2.63.

[21] Fudholi, A., Razali, N. F. M., Yazdi, M. H., Ibrahim, A., Ruslan, M. H., Othman, M. Y., & Sopian, K. (2019). TiO2/water-based photovoltaic thermal (PVT) collector: Novel theoretical approach. Energy, 183, 305–314. doi:10.1016/j.energy.2019.06.143.

[22] Prasetyo, S. D., Prabowo, A. R., & Arifin, Z. (2023). The use of a hybrid photovoltaic/thermal (PV/T) collector system as a sustainable energy-harvest instrument in urban technology. Heliyon, 9(2), e13390. doi:10.1016/j.heliyon.2023.e13390.

[23] Alawi, O. A., Kamar, H. M., Mallah, A. R., Mohammed, H. A., Sabrudin, M. A. S., Newaz, K. M. S., Najafi, G., & Yaseen, Z. M. (2021). Experimental and theoretical analysis of energy efficiency in a flat plate solar collector using monolayer graphene nanofluids. Sustainability (Switzerland), 13(10), 5416. doi:10.3390/su13105416.

[24] Çiftçi, E., Khanlari, A., Sözen, A., Aytaç, İ., & Tuncer, A. D. (2021). Energy and exergy analysis of a photovoltaic thermal (PVT) system used in solar dryer: A numerical and experimental investigation. Renewable Energy, 180, 410–423. doi:10.1016/j.renene.2021.08.081.

[25] Hai, T., & Zhou, J. (2023). Predicting the performance of thermal, electrical and overall efficiencies of a nanofluid-based photovoltaic/thermal system using Elman recurrent neural network methodology. Engineering Analysis with Boundary Elements, 150, 394-399. doi:10.1016/j.enganabound.2023.02.013.

[26] Baranwal, N. K., & Singhal, M. K. (2021). Modeling and Simulation of a Spiral Type Hybrid Photovoltaic Thermal (PV/T) Water Collector Using ANSYS. Advances in Clean Energy Technologies, Springer. doi:10.1007/978-981-16-0235-1_10.

[27] Rosli, M. A. M., Ping, Y. J., Misha, S., Akop, M. Z., Sopian, K., Mat, S., Al-Shamani, A. N., & Saruni, M. A. (2018). Simulation study of computational fluid dynamics on photovoltaic thermal water collector with different designs of absorber tube. Journal of Advanced Research in Fluid Mechanics and Thermal Sciences, 52(1), 12–22.

[28] Liu, Z., Zhang, Y., Zhang, L., Luo, Y., Wu, Z., Wu, J., Yin, Y., & Hou, G. (2018). Modeling and simulation of a photovoltaic thermal-compound thermoelectric ventilator system. Applied Energy, 228, 1887–1900. doi:10.1016/j.apenergy.2018.07.006.

[29] Gomaa, M. R., Ahmed, M., & Rezk, H. (2022). Temperature distribution modeling of PV and cooling water PV/T collectors through thin and thick cooling cross-fined channel box. Energy Reports, 8, 1144–1153. doi:10.1016/j.egyr.2021.11.061.

[30] Pang, W., Cui, Y., Zhang, Q., & Yan, H. (2020). Enhanced electrical performance for heterojunction with intrinsic thin-layer solar cells based photovoltaic thermal system with aluminum collector. International Communications in Heat and Mass Transfer, 116, 104705. doi:10.1016/j.icheatmasstransfer.2020.104705.

[31] Yandri, E. (2019). Development and experiment on the performance of polymeric hybrid Photovoltaic Thermal (PVT) collector with halogen solar simulator. Solar Energy Materials and Solar Cells, 201, 110066. doi:10.1016/j.solmat.2019.110066.

[32] He, W., Chow, T. T., Ji, J., Lu, J., Pei, G., & Chan, L. S. (2006). Hybrid photovoltaic and thermal solar-collector designed for natural circulation of water. Applied Energy, 83(3), 199–210. doi:10.1016/j.apenergy.2005.02.007.

[33] Sutanto, B., & Indartono, Y. S. (2019). Computational fluid dynamic (CFD) modelling of floating photovoltaic cooling system with loop thermosiphon. AIP Conference Proceedings, 2062, 020011. doi:10.1063/1.5086558.

[34] Jia, Y., Ran, F., Zhu, C., & Fang, G. (2020). Numerical analysis of photovoltaic-thermal collector using nanofluid as a coolant. Solar Energy, 196, 625–636. doi:10.1016/j.solener.2019.12.069.

[35] Hasan, M. I., Rageb, A. M. A. R., & Yaghoubi, M. (2012). Investigation of a Counter Flow Microchannel Heat Exchanger Performance with Using Nanofluid as a Coolant. Journal of Electronics Cooling and Thermal Control, 02(03), 35–43. doi:10.4236/jectc.2012.23004.

[36] Rosli, M. A. M., Rou, C. J., Sanusi, N., Saleem, S. N. D. N., Salimen, N., Herawan, S. G., Abdullah, N., Permanasari, A. A., Arifin, Z., & Hussain, F. (2022). Numerical Investigation on Using MWCNT/Water Nanofluids in Photovoltaic Thermal System (PVT). Journal of Advanced Research in Fluid Mechanics and Thermal Sciences, 99(1), 35–57. doi:10.37934/arfmts.99.1.3557.

[37] Dubey, S., Sarvaiya, J. N., & Seshadri, B. (2013). Temperature dependent photovoltaic (PV) efficiency and its effect on PV production in the world - A review. Energy Procedia, 33, 311–321. doi:10.1016/j.egypro.2013.05.072.

[38] Özakın, A. N., & Kaya, F. (2020). Experimental thermodynamic analysis of air-based PVT system using fins in different materials: Optimization of control parameters by Taguchi method and ANOVA. Solar Energy, 197, 199–211. doi:10.1016/j.solener.2019.12.077.

[39] Fan, W., Kokogiannakis, G., & Ma, Z. (2018). A multi-objective design optimisation strategy for hybrid photovoltaic thermal collector (PVT)-solar air heater (SAH) systems with fins. Solar Energy, 163, 315–328. doi:10.1016/j.solener.2018.02.014.

[40] Arifin, Z., Suyitno, S., Tjahjana, D. D. D. P., Juwana, W. E., Putra, M. R. A., & Prabowo, A. R. (2020). The effect of heat sink properties on solar cell cooling systems. Applied Sciences (Switzerland), 10(21), 1–16. doi:10.3390/app10217919.

[41] Mohamed, M. H., Ali, A. M., & Hafiz, A. A. (2015). CFD analysis for H-rotor Darrieus turbine as a low speed wind energy converter. Engineering Science and Technology, an International Journal, 18(1), 1–13. doi:10.1016/j.jestch.2014.08.002.

[42] Setyohandoko, G., Sutanto, B., Rachmanto, R. A., Dwi Prija Tjahjana, D. D., & Arifin, Z. (2020). A numerical approach to study the performance of photovoltaic panels by using aluminium heat sink. Journal of Advanced Research in Fluid Mechanics and Thermal Sciences, 70(2), 97–105. doi:10.37934/ARFMTS.70.2.97105.